Supplementary information

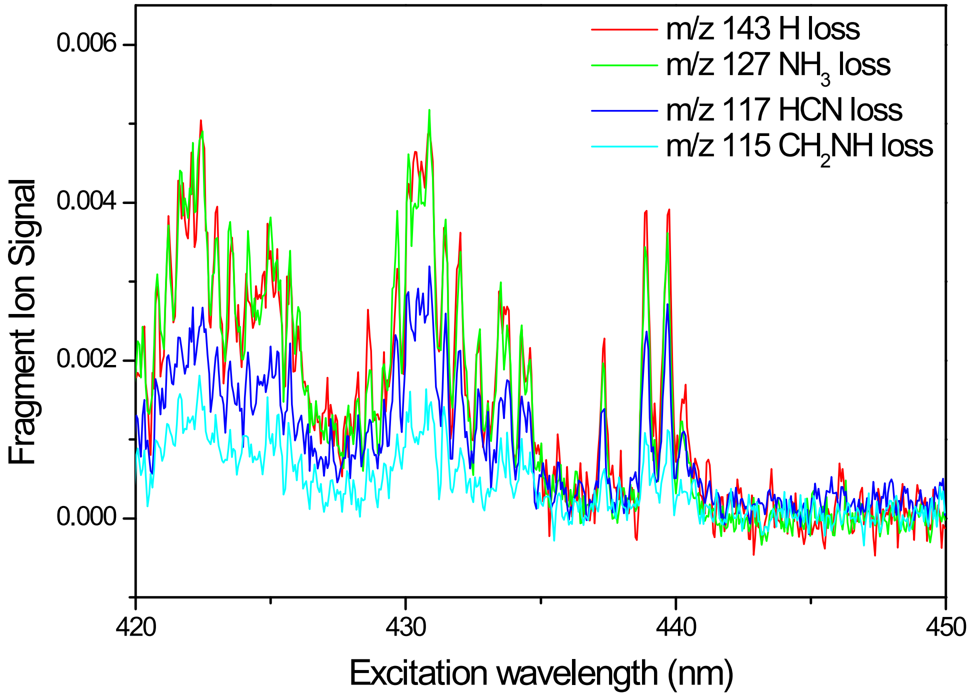

Figure SI-1: Photofragmentation spectra recorded on different fragments in the first band system of 1-ANpH$^+$ around 440 nm, showing that the branching ratio between the m/z 115/117/127/143 fragmentation channels is 1/2/3/3.

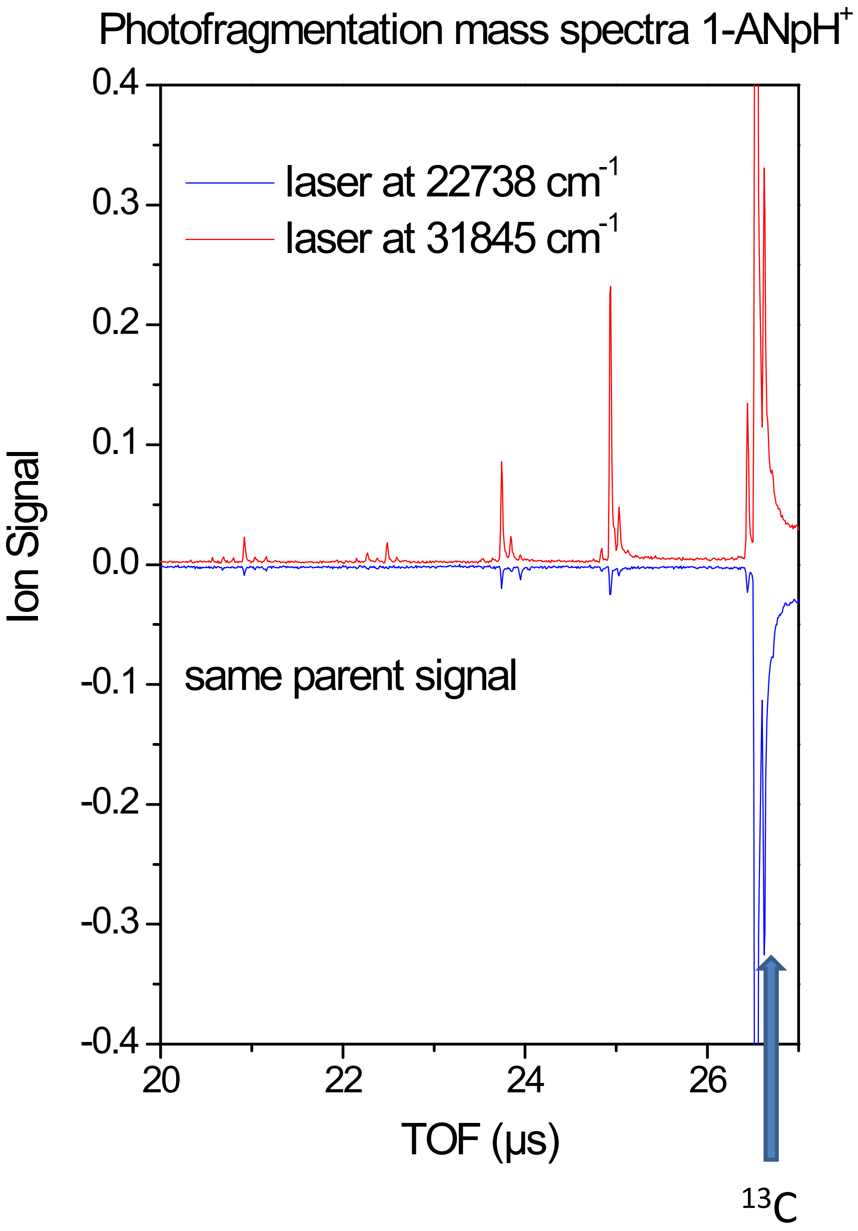

Figure SI-2: 1-ANpH+ photofragmentation mass spectra. Red trace: excitation of the 0-0 band of the D1 band system; bleu trace: excitation of the 0-0 band of the A1 band system. The intensity of the parent ion is saturated in the spectra but is deduced from the intensity of the parent ion containing one ^{13}C atom (blue arrow), which represents 10% of the ion containing only ^{12}C atoms. For the D1 band system the fragment ion signal represents ~15% of the parent signal whereas it represents only ~ 2% when the A1 band system is excited. This makes the hole burning experiment on the A1 /B1 band systems unfeasible with our experimental setup.

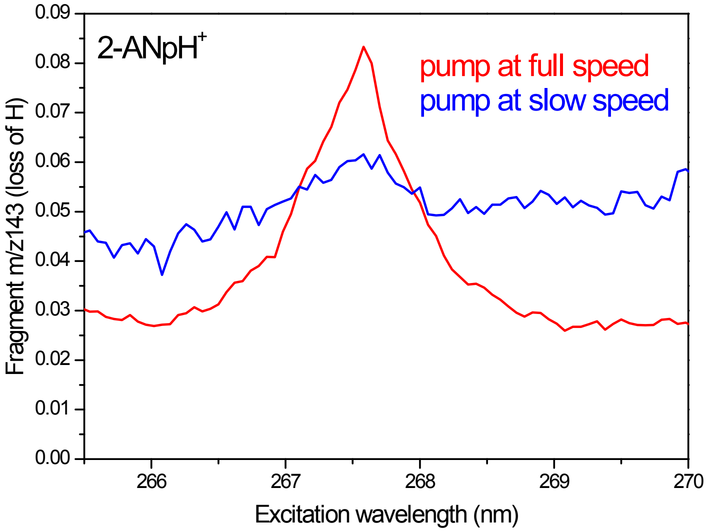

Figure SI-3: 2-ANpH⁺ photofragmentation spectrum in the UV spectral region of the D2 band: effect of decreasing the pumping speed (i.e. increasing the pressure) in the ion formation region: In red, low pressure conditions, both the background due to the 2-ANpNH$_3^+$ tautomer and the D2 band at 267 nm are observed; in blue, high pressure conditions, the 267 nm band disappears and the background increases, which means that the D2 band system does not correspond to an excited state of the 2-ANpNH$_3^+$ tautomer. As it was observed by others groups[9-12] we have also tried to modify the tautomer distribution by changing the pH of the solution, the water/ methanol ratio (from pure methanol to 20% methanol/80% water), the solvent (acetonitrile instead of water/methanol), the voltages on the needle and on the skimmer, but no strong and reproducible tautomer distribution change was observed.

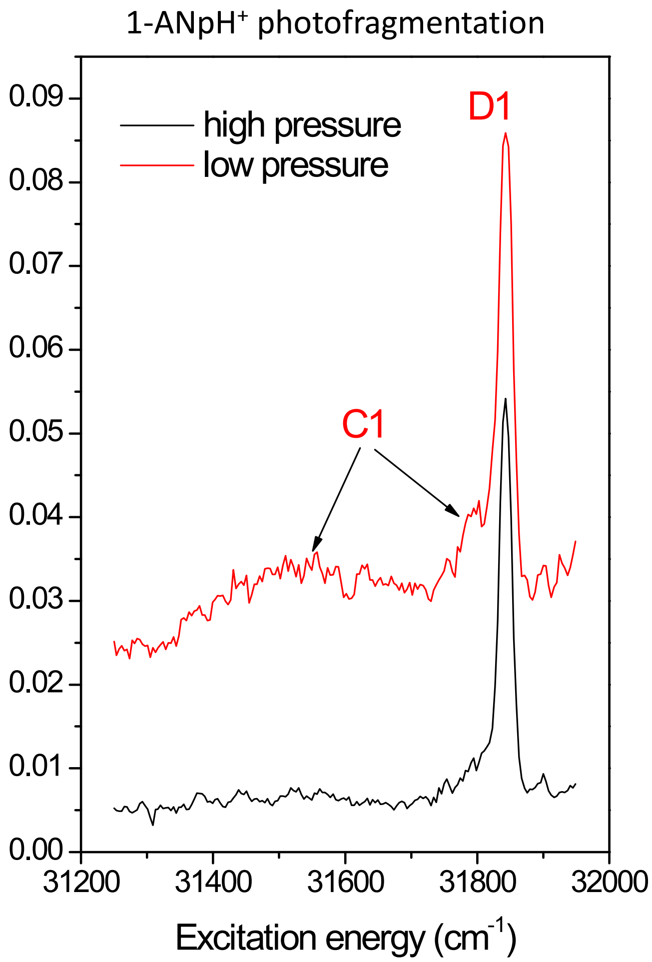

Figure SI-4: 1-ANpH$^+$ photofragmentation spectra under different pressure conditions in the first octopole chamber: black trace: under high pressure conditions, nearly only the ions protonated on the amino group (1-ANpNH$_3$$^+$) are observed (D1 band system); red trace: under lower pressure conditions, the background assigned to the 1-ANpC$_n$H$_2$$^+$ tautomers and the C1 bands assigned to the S$_2$ state of 1-ANpC$_n$H$_2$$^+$ are observed. It should be reminded that in both cases the ion are excited in the trap after cryogenic cooling so that the bands appearing at low pressure cannot be hot bands.

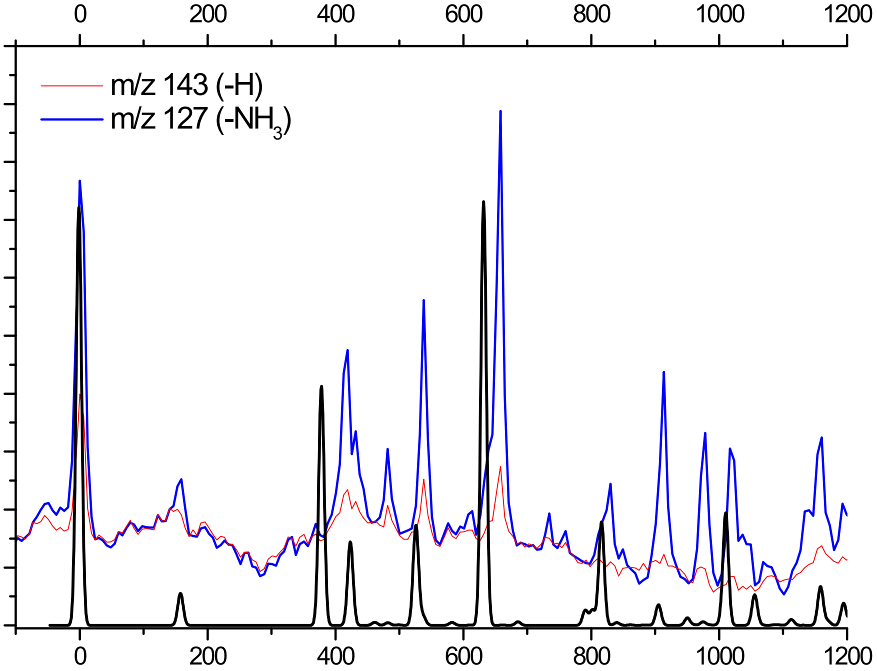

Figure SI-5: Franck Condon simulation of the first excited state of the 1-ANpNH$_3^+$ tautomer (obtained using the Pgopher program) compared to the experimental photofragmentation spectrum.

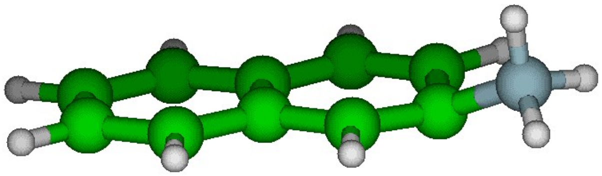

Figure SI-6: optimized structure of the 2-ANpNH$_3^+$ S$_1$ state calculated at the CC2/aug-cc-pVDZ level. The ammonium group is slightly out of the naphthalene plane by 24°.

Cartesian coordinate of the structure above

```
ATOM                      CARTESIAN COORDINATES
    1 c      -0.03237626647460      0.09295118508548      0.01886026215097
    2 c      -0.10249855734972      0.19259376721050      2.70265055076771
    3 c       2.29804003945061     -0.06849833538860     -1.35743673585278
    4 c       4.68397747486221     -0.13083661528096     -0.00584351228890
    5 c       2.33852138400495     -0.13966551106242     -4.05848632755360
    6 h       0.56905298765013     -0.08399262607070     -5.12850198931318
    7 c       7.02194143835557     -0.33875175091409     -1.31536065729741
    8 h       8.77753027802044     -0.54407179763194     -0.23019803727113
    9 c       4.66231551952435     -0.31126091068176     -5.35659497028840
   10 h       4.65025822049470     -0.28120996077809     -7.43099384434985
   11 c       6.98251238547425     -0.65221729762236     -4.02310621736102
   12 n       9.33253814820944      0.19441807245318     -5.37729548294762
   13 c       2.20332917266613      0.13059554005356      4.00712453048840
   14 c       4.56026959634376     -0.03108564850672      2.67148689996979
   15 h       6.32169058283750     -0.08088552649927      3.76283729991732
   16 h       2.24278301775756      0.20768095259240      6.07407526899866
   17 h      -1.90058026239914      0.31470656848563      3.70897896369729
   18 h       9.21633557954636     -0.17755894483688     -7.28343006161966
   19 h      -1.80247979280076      0.13505675887722     -1.05759368125755
   20 h      10.88418153253196     -0.76079644884641     -4.70450733749599
   21 h       9.69335385620823      2.12030992845785     -5.14511351326717
```

Figure SI-7: orbitals involved in the two first electronic transitions in the 1-ANpC$_4$H$_2^+$ and 1-ANpNH$_3^+$ tautomers.

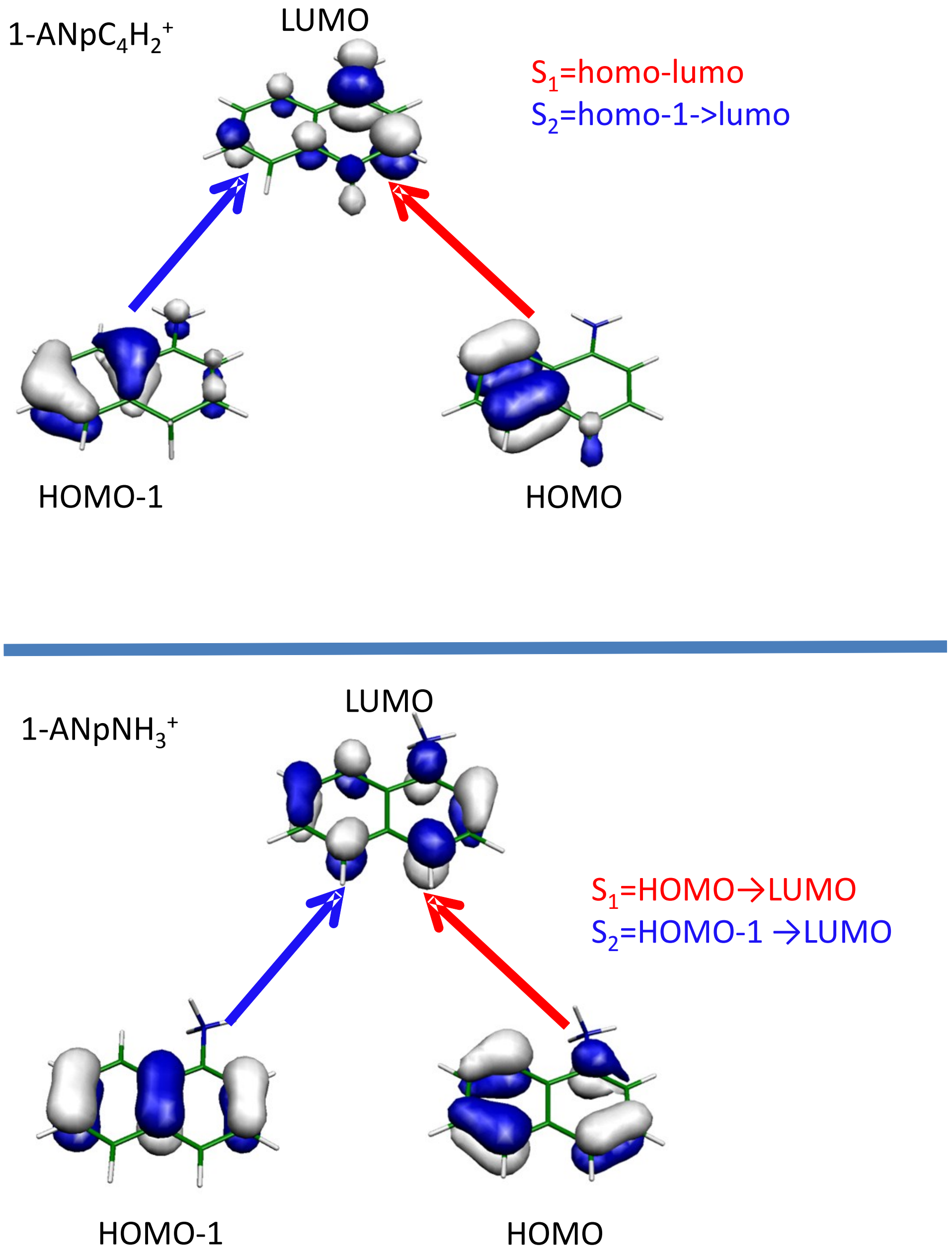

Figure SI-8: orbitals involved in the two first electronic transitions in the 2-ANpC$_1$H$_2^+$ and 2-ANpNH$_3^+$ tautomers.

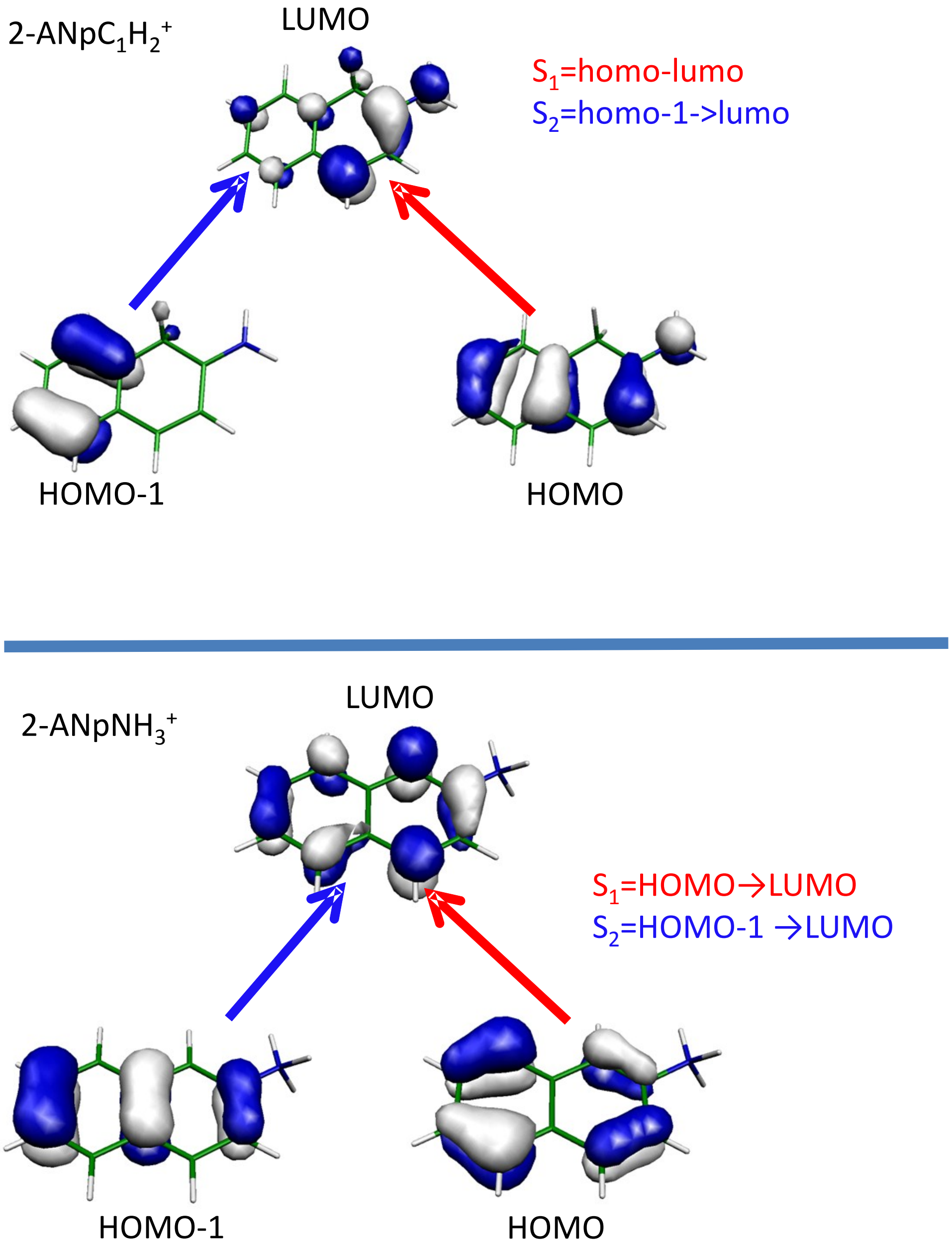

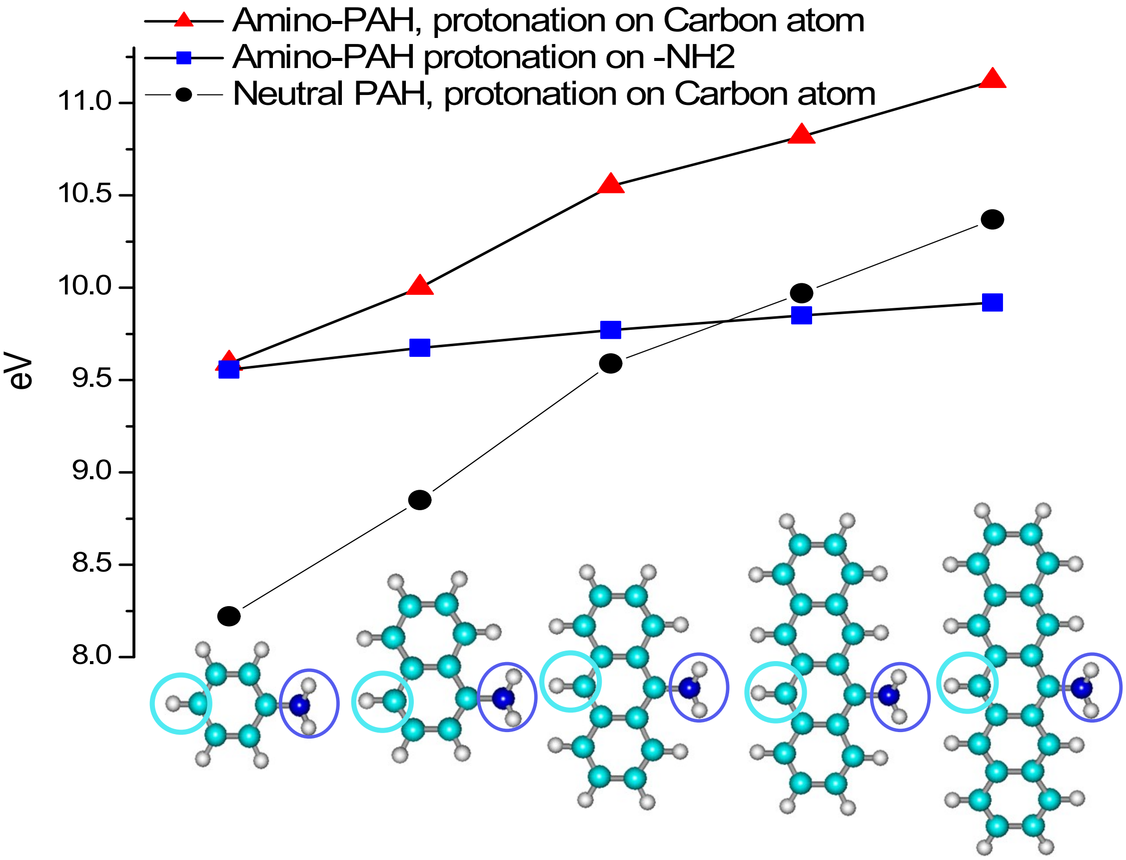

Figure SI-9: Evolution of proton affinities (PA) with the molecular size; in addition to figure 6 in the manuscript, the PA of protonated unsubstituted PAH (black circles) has been added. For homogeneity, the PA values of neutral PAHs reported in this figure have been calculated using the same method as for the amino aromatic molecules, DFT/B3LYP/cc-pVDZ.:

Table SI-1: Relative ground state energies calculated at different levels of theory for different 1- and 2-ANpH$^+$ tautomers (cc-pVDZ basis set). The energies are relative to the ground state energy of the 1-ANpNH$_3^+$ or 2-ANpNH$_3^+$ tautomer. All energies are in eV (cm^{-1}, in parenthesis). We report all eV values to the nearest 0.01 eV and all wavenumber values to the nearest 5 cm^{-1}.

	1-ANpNH$_3^+$	1-ANpC$_2$H$_2^+$	1-ANpC$_3$H$_2^+$	1-ANpC$_4$H$_2^+$	1-ANpC$_5$H$_2^+$	1-ANpC$_6$H$_2^+$	1-ANpC$_7$H$_2^+$	1-ANpC$_8$H$_2^+$
DFT	0 *0*	-0.14 *(-1130)*	+0.80 *(+6450)*	-0.33 *(-2660)*	+0.39 *(+3150)*	+0.80 *(+6450)*	+0.42 *(+3390)*	+0.62 *(+5000)*
CC2	0	+0.07		-0.12				
CCSD(T)	0	-0.032 *(-255)*		-0.21 *(-1715)*				
MP2	0	+0.17		-0.01				
MP4	0	0.009 *(+75)*		-0.17 *(-1360)*				

	2-ANpNH$_3^+$	2-ANpC$_1$H$_2^+$	2-ANpC$_3$H$_2^+$	2-ANpC$_4$H$_2^+$	2-ANpC$_5$H$_2^+$	2-ANpC$_6$H$_2^+$	2-ANpC$_7$H$_2^+$	2-ANpC$_8$H$_2^+$
DFT	0 *0*	-0.31 *(-2500)*	+0.28 *(+2260)*	0.67 *(+5400)*	+0.57 *(+4600)*	+0.07 *(+565)*	+0.68 *(+5480)*	+0.06 *(+485)*
CC2	0	-0.09				+0.37	+1.04	+0.36
CCSD(T)	0	-0.14 *(-1170)*				+0.26 *(+2060)*		+0.29 *(+2370)*
MP2	0	+0.03				+0.57	+1.11	+0.57
MP4	0	-0.11 *(-865)*				+0.32 *(+2555)*		+0.35 *(+2815)*

As seen above, the 1-ANpC$_4$H$_2^+$ tautomer is always found more stable than the 1-ANpNH$_3^+$ tautomer. The 1-ANpC$_2$H$_2^+$ is more stable than 1-ANpNH$_3^+$ with DFT and almost isoenergetic with 1-ANpNH$_3^+$ using CCSD(T) or MP4 methods. For 2-ANpH$^+$, the 2-ANpC$_1$H$_2^+$ tautomer is more stable than the 2-ANpNH$_3^+$ tautomer, while the 2-ANpC$_6$H$_2^+$ and 2-ANpC$_8$H$_2^+$ tautomers are always less stable than the 2-ANpNH$_3^+$ tautomer. As already noted in previous reports [1], MP2 (see table SI-1) method overestimates the stability of the NH$_3^+$ tautomer as compared to the C$_n$H$_2^+$ tautomers, while DFT, MP4 and CCSD(T) methods provide consistent results.

Table SI-2: Calculated frequencies at the CC2/aug-cc-pVDZ level of the first excited state of 1-ANpNH$_3^+$ and tentative assignment of the bands observed

Mode number	Calculated frequencies		Observed frequencies	tentative assignment
1	80	NH$_3$ rotation		
2	136	NH$_3$ rotation		
3	152	Ring deformation out of plane		
			159 (2*80)	1_0^2
4	163	Ring deformation out of plane		
5	249	NH$_3$ bending in plane		
6	302	Ring deformation out of plane		
7	354	Ring deformation out of plane		
8	379	Ring deformation in plane	419	8_0^1
9	404	Ring deformation out of plane		
10	420	Ring deformation out of plane		
11	424	Ring deformation in plane	482	11_0^1
12	463	Ring deformation in plane		
13	527	Ring deformation in plane	538	13_0^1
14	531	C2H out of plane		
15	583	Ring deformation out of plane		
16	633	Ring breathing in plane	658	16_0^1
17	684	CH out of plane		
18	736	CH out of plane		
19	752	CH out of plane		
20	755	Ring deformation in plane		
21	817	Ring in plane	830	21_0^1
22	832	CH out of plane		
23	853	CH out of plane		
24	874	CH out of plane		
25	907	Ring deformation in plane		
			914	$8_0^1 13_0^1$
			978	$11_0^1 13_0^1$
26	992	ring in plane		
			1017	$8_0^1 16_0^1$

27	1025	NH/CH in plane		
28	1040	NH_3 out of plane		
29	1044	NH &CH bend in plane		
30	1108	CH bend in plane		
31	1137	CH bend in plane		
32	1150	CH bend in plane		
			1160	$13^1_0 16^1_0$
			1196	
33	1207	CH bend in plane		
			1219	$8^1_0 21^1_0$
34	1228	CH bend in plane		
35	1242	CH bend in plane		
36	1344	CH bend in plane		
			1351	
37	1384	CH bend in plane		
			1390	
38	1408	CH bend in plane		
39	1427	CH bend in plane & NH_3 umbrella		
40	1444	CH bend in plane & ring deformation		
			1450	
41	1470	Ring deformation in plane & NH_3 umbrella		
42	1479	NH_3 umbrella		
43	1489	Ring deformation in plane		
			1497	
			1550	
44	1618	NH_3 antisymmetric bend		
45	1618	NH symmetric +ring deformation in plane		
46	1632	NH symmetric bend		
47	1659	NH symmetric +ring deformation in plane		
48	3171	CH stretch		
49	3202	CH stretch		
50	3204	CH stretch		
51	3208	CH stretch		
52	3217	CH stretch		
53	3230	CH stretch		
54	3242	CH stretch		
55	3335	NH_3 stretch symmetric		
56	3413	NH_3 stretch antisymmetric		
57	3479	NH_3 stretch antisymmetric		

Table SI-3: Comparison of the calculated tautomer stability for ions isolated in the gas phase or ions in solution calculated using COSMO (COnductor-like Screening Model) as implemented in the Turbomole package. The calculations indicate that the tautomer protonated on the amino group is the most stable in solution, whereas protonation on a carbon atom (C4 for 1-ANpH$^+$ and C1 for 2-ANpH$^+$) is favored for isolated molecules.

	DFT	DFT+COSMO (ε=80)
1-ANpNH$_3^+$	0	0
1-ANpC$_2$H$_2^+$	-0.14	+0.35
1-ANpC$_4$H$_2^+$	-0.33	+0.22
2-ANpNH$_3^+$	0	0
2-ANpC$_1$H$_2^+$	-0.31	+0.24

Energetics of the dissociation channels

The energetics of the dissociation channels has been calculated at the DFT level and is summarized in figure 5 together with the energy of the observed excited states. (The details of the calculations can be found in the table SI-4)

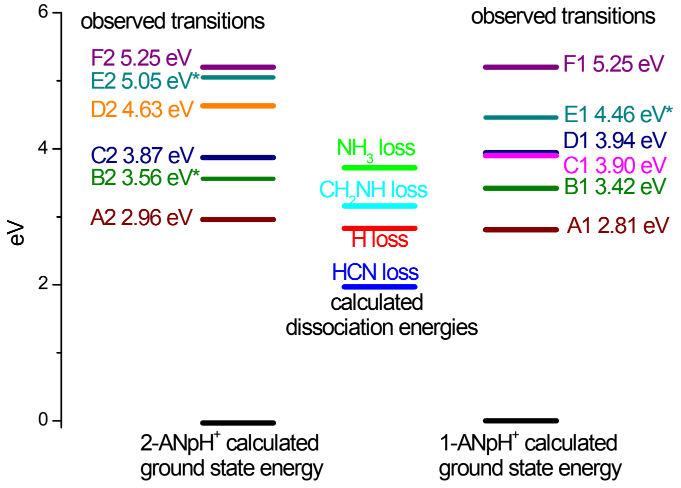

Vertical transition energies are marked with a star *

Figure 5: Comparison between the energy of the electronic transitions and the energy of the dissociation channels.

The lower dissociation energy corresponds to the HCN loss channel, well under the energy of the first band system, while the NH_3 loss channel has the highest dissociation energy, slightly under the energy of the most intense band system D1 and C2. It should be noted that the H loss channel as well as the NH_3 loss channel are simple bond cleavage for aminonaphthalene protonated on the amino group. On the other hand, the other dissociation channels necessitate rearrangement processes involving barriers higher than the dissociation energy. As in protonated aminopyrene[1] , the NH_3 loss channel is higher in energy than the H loss channel by almost 1 eV.

Note that the HCN loss channel is observed for the low energy band systems (A1, B1 and A2), but absent when exciting the D1 and C2 major band systems. In protonated diazine and aminopyridine[2] the HCN loss channel mechanism involves a hydrogen or proton transfer to a carbon atom, and if the same mechanism is assumed for ANpH$^+$, the most probable parents will be the ANpC$_n$H$_2^+$ tautomers. This would therefore mean that the D1 and C2 band systems correspond to 1-and 2-ANpNH$_3^+$ tautomers. These assumptions may be checked by comparison with calculations of the excited state transitions.

Table SI-4: Energetics of the dissociation channels

	Energy DFT/B3lyp (hartree)	**Proton affinity (eV)**		Energy DFT/B3lyp (hartree)	
1-ANp mass 143	-440.9942406			-440.99413893	2-ANp mass 143
1-ANpH$^+$ m/z 144	-441.3497544	9.67	9.71	-441.35092526	2-ANpH$^+$ m/z 144
		Dissociation Energy (eV)			
HCN loss channel m/z 117 + 27 (HCN)	-347.899-93.378 =-441.277	1.97	2.00	-347.899-93.378 =-441.277	HCN loss channel m/z 117 + 27 (HCN)
H loss channel m/z 143 (1-ANp$^+$) +1 (H)	-440.7476-0.4983 =-441.2459	2.83	2.87	-440.7472-0.4983 =-441.2455	H loss channel m/z 143 (2-ANp$^+$) +1 (H)
CH$_2$NH loss channel m/z 115+29 (CH$_2$NH)	-346.659-94.574 =-441.233	3.16	3.19	-346.659-94.574 =-441.233	CH$_2$NH loss channel m/z 115+29 (CH$_2$NH)
NH$_3$ loss channel m/z 127 +17 (NH$_3$)	-384.695-56.518 =-441.213	3.72	3.84	-384.692-56.518 =-441.210	NH$_3$ loss channel m/z 127 +17 (NH$_3$)

References

(1) Noble, J. A.; Dedonder-Lardeux, C.; Mascetti, J.; Jouvet, C. Electronic Spectroscopy of Protonated 1-Aminopyrene in a Cold Ion Trap. *Chem. - An Asian J.* **2017**, *125*, 1523–1531.

(2) Broquier, M.; Soorkia, S.; Dedonder-Lardeux, C.; Jouvet, C.; Theulé, P.; Grégoire, G. Twisted Intramolecular Charge Transfer in Protonated Amino Pyridine. *J. Phys. Chem. A* **2016**, *120* (21), 3797–3809.